

Majorana Edge States in Superconductor/Noncollinear Magnet Interfaces

Wei Chen^{1,2} and Andreas P. Schnyder²

¹*Theoretische Physik, ETH-Zürich, CH-8093 Zürich, Switzerland*

²*Max-Planck-Institut für Festkörperforschung, Heisenbergstrasse 1, D-70569 Stuttgart, Germany*

(Dated: March 25, 2022)

Through $s-d$ coupling, a superconducting thin film interfaced to a noncollinear magnetic insulator inherits its magnetic order, which may induce unconventional superconductivity that hosts Majorana edge states. From the cycloidal, helical, or (tilted) conical magnetic order of multiferroics, or the Bloch and Neel domain walls of ferromagnetic insulators, the induced pairing is $(p_x + p_y)$ -wave, a pairing state that supports Majorana edge modes without adjusting the chemical potential. In this setup, the Majorana states can be separated over the distance of the long range magnetic order, which may reach macroscopic scale. A skyrmion spin texture, on the other hand, induces a $(p_r + ip_\varphi)$ -wave-like state, which albeit nonuniform and influenced by an emergent electromagnetic field, hosts both a bulk persistent current and a topological edge current.

PACS numbers: 73.20.-r, 71.10.Pm, 73.21.-b, 74.45.+c

Introduction.- Motivated by possible applications in non-abelian quantum computation [1], the search for Majorana fermions in condensed matter systems has witnessed a boost recently [2–6]. Indeed there has been much effort to design and fabricate one-dimensional heterostructures in which topological p -wave superconductivity is proximity induced [7–12]. One particularly promising proposal are chains of magnetic atoms with noncollinear spin texture on the surface of a conventional superconductor (SC) [13–22]. The presence of these magnetic adatoms induces Shiba bound states [23–25], whose low-energy physics is equivalent to a one-dimensional (1D) p -wave SC with Majorana modes at its ends. Scanning tunneling measurements of zero-bias peaks at the ends of Fe chains deposited on superconducting Pb have been interpreted as evidence of Majorana modes [26], although no general consensus has been reached regarding the definitive existence of Majorana states in these systems [27].

Since thin films are generally easier to manufacture than adatoms, it is intriguing to ask if such 1D proposals can be generalized to two-dimensional (2D) systems, where a superconducting thin film is coupled to a noncollinear magnet. The work by Nakosai *et al.* [28] first shed light on this issue. It was found that a spiral spin texture in proximity to an s -wave superconductor induces a $(p_x + p_y)$ -wave state, while a skyrmion crystal spin configuration gives rise to $(p_x + ip_y)$ -wave-like pairing. The former pairing state exhibits bulk nodes and Majorana flat-band edge states, whereas the latter one is characterized by a full gap with chirally dispersing Majorana edge states that carry a quantized Hall current. In this Letter, we show that these phenomena occur in a much broader class of superconductor/noncollinear magnet interfaces. In particular, we find that a great variety of noncollinear magnets, including multiferroic insulators with helical, cycloidal, and (tilted) conical order, as well as magnetic domain walls of ferromagnetic (FM)

insulators, interfaced with an s -wave superconductor induce a $(p_x + p_y)$ -wave pairing state with Majorana flat bands at the boundary. We derive the general criterion for the Majorana edge state for any wave length and direction of the noncollinear magnetic order, show that the Majorana modes occur without fine-tuning of the chemical potential, and demonstrate that the translation invariance along the direction perpendicular to the noncollinear order greatly enhances the chance to observe Majorana states. Furthermore, we investigate a single skyrmion spin texture coupled to an s -wave superconductor and shown that at this interface an inhomogeneous $(p_r + ip_\varphi)$ -wave-like pairing is induced, which coexists with the emerging electromagnetic field resulted from the noncoplanar spin texture.

SC/multiferroic interface.- Evidence from the T_c reduction in magnetic oxide/SC heterostructures [29, 30] suggests that $s-d$ coupling $\Gamma \mathbf{S}_i \cdot \boldsymbol{\sigma}$ generally exists at the interface atomic layer between an SC and an insulating magnetic oxide [31], where $\boldsymbol{\sigma}$ is the conduction electron spin and \mathbf{S}_i the local moment. This leads us to consider the following model for the SC/multiferroic interface, which is the 2D generalization of the 1D proposals of Refs. 13, 14,

$$H = \sum_{i,\delta,\alpha} t_{i\delta} f_{i\alpha}^\dagger f_{i+\delta\alpha} + t_{i\delta}^* f_{i+\delta\alpha}^\dagger f_{i\alpha} - \mu \sum_{i,\alpha} f_{i\alpha}^\dagger f_{i\alpha} + \sum_{i,\alpha,\beta} (\mathbf{B}_i \cdot \boldsymbol{\sigma})_{\alpha\beta} f_{i\alpha}^\dagger f_{i\beta} + \sum_i \Delta_0 \left(f_{i\uparrow}^\dagger f_{i\downarrow}^\dagger + f_{i\downarrow} f_{i\uparrow} \right), \quad (1)$$

where $i = \{i_x, i_y\}$ is the site index, $\hat{\boldsymbol{\delta}} = \{\hat{\mathbf{a}}, \hat{\mathbf{b}}\}$ is the planar unit vector, and α is the spin index. In the absence of spin-orbit interaction, the majority of the noncollinear order discovered in multiferroics, for instance in perovskite rare earth manganites [32–35], can be generically described by the conical order

$$\mathbf{B}_i = (B_i^x, B_i^y, B_i^z) = (B_{\parallel} \sin \theta_i, B_{\perp}, B_{\parallel} \cos \theta_i), \quad (2)$$

as far as their effect on the SC is concerned, since the choice of coordinate for $\boldsymbol{\sigma}$ is arbitrary. For instance, cycloidal and helical order are equivalent by trivially exchange two components of $\boldsymbol{\sigma}$, and conical orders with any tilting angle are equivalent. Here $B_{\parallel} = \Gamma|\mathbf{S}_{i\parallel}|$ and $B_{\perp} = \Gamma|\mathbf{S}_{i\perp}|$ are the planar and out-of-plane components of the local moment, and the planar angle $\theta_i = \mathbf{Q} \cdot \mathbf{r}_i$ is determined by the spiral wave vector \mathbf{Q} and the planar position \mathbf{r}_i . The cycloidal order is the case when $B_{\perp}\hat{\mathbf{y}} = 0$. Note that a three-dimensional conical order projected to a surface cleaved at any direction is still that described by Eq. (2), so our formalism is applicable to a thin film or the surface of a single crystal multiferroic in any crystalline orientation, assuming no lattice mismatch with the SC and a constant $|\mathbf{S}_i| = |\mathbf{S}|$.

We perform two consecutive rotations to align the \mathbf{B}_i field along σ^z ,

$$\begin{aligned} \begin{pmatrix} f_{i\uparrow} \\ f_{i\downarrow} \end{pmatrix} &= \begin{pmatrix} \cos \frac{\theta_i}{2} & -\sin \frac{\theta_i}{2} \\ \sin \frac{\theta_i}{2} & \cos \frac{\theta_i}{2} \end{pmatrix} \begin{pmatrix} \cos \frac{\gamma}{2} & i \sin \frac{\gamma}{2} \\ i \sin \frac{\gamma}{2} & \cos \frac{\gamma}{2} \end{pmatrix} \begin{pmatrix} g_{i\uparrow} \\ g_{i\downarrow} \end{pmatrix} \\ &= U_i \begin{pmatrix} g_{i\uparrow} \\ g_{i\downarrow} \end{pmatrix}, \end{aligned} \quad (3)$$

where $\sin \gamma = B_{\perp}/B_0$ and $B_0 = \sqrt{B_{\parallel}^2 + B_{\perp}^2} = |\Gamma\mathbf{S}|$, under which one obtains

$$\begin{aligned} H &= \sum_{i,\delta,\alpha,\beta} t_{i\delta} \Omega_{i\delta\alpha\beta} g_{i\alpha}^{\dagger} g_{i+\delta\beta} + t_{i\delta}^* (\Omega_{i\delta}^*)_{\beta\alpha} g_{i+\delta\alpha}^{\dagger} g_{i\beta} \\ &+ \sum_{i,\alpha,\beta} (B\sigma_{\alpha\beta}^z - \mu I_{\alpha\beta}) g_{i\alpha}^{\dagger} g_{i\beta} + \sum_i \Delta_0 (g_{i\uparrow}^{\dagger} g_{i\downarrow}^{\dagger} + g_{i\downarrow} g_{i\uparrow}), \\ \Omega_{i\delta} &= U_i^{\dagger} U_{i+\delta} = \begin{pmatrix} \alpha_{i\delta} & -\beta_{i\delta}^* \\ \beta_{i\delta} & \alpha_{i\delta}^* \end{pmatrix}, \\ \alpha_{i\delta} &\equiv \alpha_{\delta} = \cos \frac{\mathbf{Q} \cdot \boldsymbol{\delta}}{2} - i \sin \gamma \sin \frac{\mathbf{Q} \cdot \boldsymbol{\delta}}{2}, \\ \beta_{i\delta} &\equiv \beta_{\delta} = \cos \gamma \sin \frac{\mathbf{Q} \cdot \boldsymbol{\delta}}{2}. \end{aligned} \quad (4)$$

In what follows, we consider hopping to be real and isotropic $t_{i\delta} = t_{i\delta}^* = t$.

In the limit $B_0 \approx |\mu| \gg \{t, \Delta_0\}$ with $\mu < 0$, one can construct an effective low energy theory for the spin species near the Fermi level, which is the spin down band. This is done by introducing a unitary transformation $H' = e^{-iS} H e^{iS}$ to eliminate the spin mixing terms order by order [13]. At first order, the pairing part

$$H_{\text{eff},\Delta} = \sum_{i,\delta} \left[\left(\frac{1}{B} - \frac{1}{\mu} \right) \Delta_0 t \beta_{i\delta}^* g_{i\downarrow} g_{i+\delta\downarrow} + \text{h.c.} \right] \quad (5)$$

resembles a spinless p -wave superconductor with anisotropic nearest-neighbor and next-nearest-neighbor hopping. From Eq. (4) one has $\beta_{i\delta}^* = \cos \gamma \sin \mathbf{Q} \cdot \boldsymbol{\delta}/2$, so the induced pairing is of $(p_x + p_y)$ -wave symmetry, with the magnitude of the gap determined by the wave length of the planar component of the conical order.

To derive the criterion for the appearance of Majorana edge states, we introduce Majorana fermions $g_{i\sigma} = \frac{1}{2}(b_{i1\sigma} + ib_{i2\sigma})$, $g_{i\sigma}^{\dagger} = \frac{1}{2}(b_{i1\sigma} - ib_{i2\sigma})$ with $\{b_{im\alpha}, b_{i'm'\beta}\} = 2\delta_{ii'}\delta_{mm'}\delta_{\alpha\beta}$, and express the Hamiltonian $H = (i/4) \sum_{\mathbf{q}} b_{\mathbf{q}}^{\dagger} A(\mathbf{q}) \mathbf{b}_{-\mathbf{q}}$ in terms of the basis $b_{\mathbf{q}}^{\dagger} = (b_{\mathbf{q}1\uparrow}, b_{\mathbf{q}1\downarrow}, b_{\mathbf{q}2\uparrow}, b_{\mathbf{q}2\downarrow})$ [14]. We choose open boundary condition (OBC) along $\hat{\mathbf{x}}$ and periodic one (PBC) along $\hat{\mathbf{y}}$, such that $-\pi < q_y < \pi$ is a good quantum number. At a particular q_y , only when q_x satisfies

$$\beta_a \sin q_x + \beta_b \sin q_y = 0, \quad (6)$$

is the Majorana Hamiltonian $A(q_x, q_y)$ skew symmetric. The two solutions q_{x1} and q_{x2} are the high symmetry points at which the Pfaffian is calculated. The topological index [14] is now a function of q_y

$$M(q_y) = \text{Sign}(\text{Pf}[A(q_{x1}, q_y)]) \text{Sign}(\text{Pf}[A(q_{x2}, q_y)]) . \quad (7)$$

When $M(q_y) = -1$, or equivalently

$$\begin{aligned} &\sqrt{\Delta_0^2 + (|\mu - 2t\bar{\alpha}_b \cos q_y| + |2t\bar{\alpha}_a \cos q_{x1}|)^2} > B \\ &> \sqrt{\Delta_0^2 + (|\mu - 2t\bar{\alpha}_b \cos q_y| - |2t\bar{\alpha}_a \cos q_{x1}|)^2}, \end{aligned} \quad (8)$$

where $\bar{\alpha}_{\delta} = (\alpha_{\delta} + \alpha_{\delta}^*)/2$, the Majorana edge state with momentum q_y appears. Setting $\bar{\alpha}_b = 0$ and $q_{x1} = 0$ recovers the well known 1D result [14].

Equation (8) is the general criterion for the Majorana state to appear at momentum q_y for any given spiral or conical order. It is supported by numerically solving the Bogoliubov-de Gennes (BdG) equation with the boundary conditions we choose. A spin-generalized Bogoliubov transformation $g_{i\sigma} = \sum_{n,\alpha} u_{in\sigma\alpha} \gamma_{n\alpha} + v_{in\sigma\alpha}^* \gamma_{n\alpha}^{\dagger}$ is introduced to diagonalize Eq. (4). Figure 1(b) shows a typical dispersion $E(n, q_y)$, which display Majorana zero-energy states in the q_y 's that satisfy Eq. (8). Note that Equation (8) can be satisfied even if $\mu = 0$, so adjusting chemical potential is generally not needed. Consequently, the edge states can occur in an isolated sample without attaching any leads. The $2t\bar{\alpha}_b \cos q_y$ factor greatly enlarges the number of q_y 's that can satisfy Eq. (8), hence increases the chance to observe Majorana Fermions, as one can see from the phase diagram shown in Fig. 1(a) that has much larger topologically nontrivial phase in the B_0 - $\bar{\alpha}$ space than the 1D cases, where the (weak) topological phase [36] is judged by whether any q_y satisfies Eq. (8) at a given $(B_0, \bar{\alpha})$.

The localized Majorana edge states can be seen as the zero bias peaks (ZBPs) in the local density of states (LDOS) along $\hat{\mathbf{x}}$ direction, as plotted in Fig. 1(c). Three gap-like features show up in the LDOS. The two symmetric in ω come from the bulk gap Δ whose position is shifted by the $s-d$ coupling $\pm B_0$ as its effect is similar to a magnetic field, and typically has a magnitude [37] $0.01 \sim 1\text{eV}$ so $B_0 > \Delta$. The gap-like feature near zero energy represents the induced $(p_x + p_y)$ -wave gap in Eq. (5).

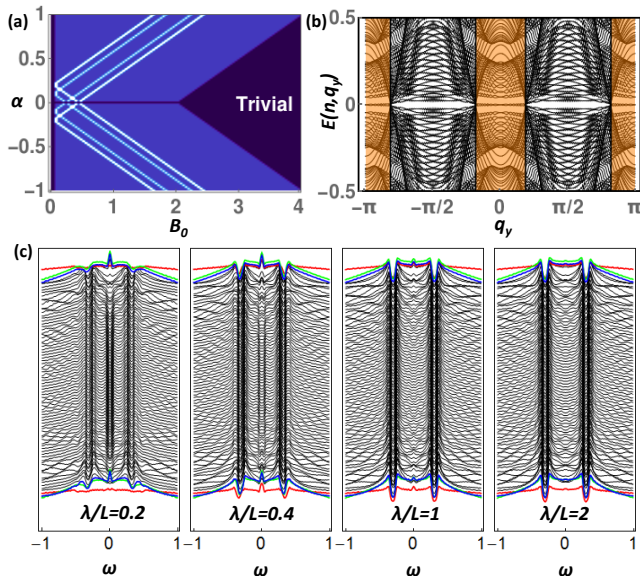


FIG. 1: (color online) (a) The topologically nontrivial phase (blue region) of the 2D model Eq. (1) with $\mu = 0$ as a function of $s - d$ coupling B_0 and $\alpha \equiv \bar{\alpha}_a$ for (1, 0) spiral. For comparison, the nontrivial phase of 1D model with $\mu = -0.2$ and -0.4 are shown as the region inside light blue dots and white dots, respectively. (b) Energy levels of a system with size $L = 80a$ subject to a spiral of wave length $\lambda = 2\pi/|\mathbf{Q}| = 16a$ at $B_0 = 0.3$. The orange regions are the q_φ 's at which the topological criterion Eq. (8) is satisfied, where one also sees the Majorana zero energy edge state. (c) the LDOS along \hat{x} for different values of λ/L . Red, green, and blue lines are the first, second, and third site away from the edge. The $\lambda/L = 2$ case represents a Neel or Bloch domain wall in a ferromagnetic insulator. Other parameters are $t = -1$, $\Delta = 0.05$.

The weight of ZBP decreases as the spiral wave length $\lambda = 2\pi/|\mathbf{Q}|$ increases. The $\lambda/L = 2$ case represents a Neel or Bloch magnetic domain wall joining two regions of opposite spin orientations in a ferromagnetic insulator, since it can be viewed as a spiral with half a wave length, and the interface to a SC can be described by Eqs. (1) to (8). In such case, the ZBP is small but still discernable.

For a thin film with finite thickness but the $s - d$ coupling only at the interface atomic layer, the Majorana state extends over few layers away from the interface, so one may need a SC film of few atomic layers thickness to observe the Majoranas by any surface probe such as scanning tunneling microscope (STM). Even if the multiferroic contains domains of different spiral chirality, or the spin texture is not perfectly periodic, the Majorana edge state still exists at the edge and the boundary between domains. The large single domain of multiferroics, currently of mm size [38], may help to separate the Majorana fermions over a distance of macroscopic scale.

SC/skyrmion interface.- Skyrmion spin textures have been observed in thin film insulating multiferroics [39, 40]

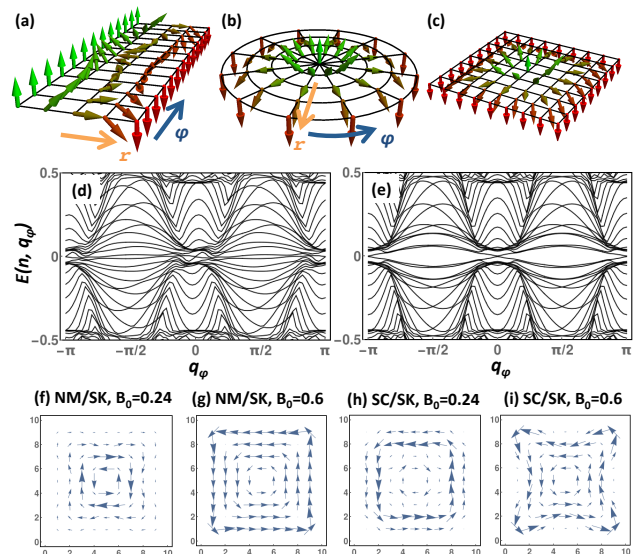


FIG. 2: (color online) (a) The spin texture of the pedagogical model, which is closely related to a single nonchiral skyrmion in (b) a polar lattice and (c) a square lattice. (d) The dispersion of the pedagogical model with OBC in \hat{r} and PBC in $\hat{\varphi}$, with $N_r = N_\varphi = 40$, and (e) if the emerging EM field is manually turned off, at $B_0 = 0.24$. The spontaneous current pattern at the interface to a single nonchiral skyrmion of size 9×9 is shown in (f), (g) for the normal state ($\Delta = 0$) and (h), (i) for the SC state. Parameters are $t = -1$, $\Delta = 0.2$, $\mu = -0.1$.

at temperatures approaching the typical SC transition temperature, with a small magnetic field that presumably has negligible effect on the SC. To gain more understanding about the SC/skyrmion insulator interface, disregarding external magnetic fields, we first consider a closely related pedagogical model defined on a square lattice, whose low-energy sector can be studied analytically. The spin texture of this model is that shown in Fig. 2(a), yielding a magnetic field on its interface to an SC

$$\mathbf{B}_i = B (\sin \theta_i \cos \varphi_i, \sin \theta_i \sin \varphi_i, \cos \theta_i) \quad (9)$$

at position (r_i, φ_i) on the square lattice, where $\theta_i = \pi r_i/R$ and R is the width in \hat{r} direction. We assume OBC along the \hat{r} direction and PBC along the $\hat{\varphi}$ direction. The Hamiltonian is described by Eq. (1) with $\hat{\delta} = \{\hat{r}, \hat{\varphi}\}$. To align the spin texture along σ^z , one performs the rotation in Eq. (3) with U_i defined by

$$U_i = \begin{pmatrix} \cos \frac{\theta_i}{2} & -\sin \frac{\theta_i}{2} e^{-i\varphi_i} \\ \sin \frac{\theta_i}{2} e^{i\varphi_i} & \cos \frac{\theta_i}{2} \end{pmatrix}, \quad (10)$$

which yields Eq. (4) with

$$\begin{aligned}\alpha_{i\varphi} &= 1 + 2ie^{i\pi/N_\varphi} \sin^2\left(\frac{\theta_i}{2}\right) \sin\frac{\pi}{N_\varphi}, \quad \alpha_{ir} = \cos\frac{\pi}{N_r}, \\ \beta_{i\varphi} &= i \sin\theta_i e^{i(\varphi_i+\varphi_{i+\varphi})/2} \sin\frac{\pi}{N_\varphi} \equiv e^{i(\varphi_i+\varphi_{i+\varphi})/2} \tilde{\beta}_{i\varphi}, \\ \beta_{ir} &= e^{i\varphi_i} \sin\frac{\pi}{N_r} \equiv e^{i\varphi_i} \tilde{\beta}_{ir},\end{aligned}\quad (11)$$

where N_r and N_φ are the number of sites in each direction. After gauging away the extra phase $\beta_{i\delta} \rightarrow \tilde{\beta}_{i\delta}$ by $e^{-i\varphi_i/2} g_{i\downarrow} \rightarrow g_{i\downarrow}$ and $e^{i\varphi_i/2} g_{i\uparrow} \rightarrow g_{i\uparrow}$, the Hamiltonian is translationally invariant along $\hat{\varphi}$ but not along \hat{r} because $\tilde{\beta}_{i\varphi} \propto \sin\theta_i = \sin(\pi r_i/R)$. In the $B \approx |\mu| \gg \{t_\delta, \Delta_0\}$ limit, using Eq. (5) of the low-energy effective theory, the induced gap along \hat{r} and $\hat{\varphi}$ are proportional to $\tilde{\beta}_{ir}^*$ and $\tilde{\beta}_{i\varphi}^*$, and therefore of $(p_r + ip_\varphi)$ -wave-like symmetry.

The spin-conserved $\alpha_{i\delta} t_{i\delta}$ and spin-flip $\beta_{i\delta} t_{i\delta}$ hopping in the $g_{i\sigma}$ basis contain an emergent electromagnetic (EM) field [41, 42] coming from the spatial dependence of the unitary transformation [43]. This becomes evident in the continuous limit $\theta_i \rightarrow \theta$, $\varphi_i \rightarrow \varphi$, $U_i \rightarrow U$, and using $\int_0^{a_r} dr \partial_r \theta = 2\pi/N_r \ll 1$ and $\int_0^{a_\varphi} d\varphi \partial_\varphi \varphi = 2\pi/N_\varphi \ll 1$. The $\{\alpha_\delta, \beta_\delta\}$ contain the phase gained over one lattice constant

$$\Omega_\delta = \begin{pmatrix} \alpha_\delta & -\beta_\delta^* \\ \beta_\delta & \alpha_\delta^* \end{pmatrix} = e^{-iq \int_0^{a_\delta} d\delta A_\delta}, \quad (12)$$

where $A_\delta = i(\hbar/q)U^\dagger \partial_\delta U$. The factor of i difference between A_r and A_φ eventually leads to the induced $(p_r + ip_\varphi)$ -wave-like gap. Figure 2(d) shows the dispersion of this pedagogical model, and Fig. 2(e) shows the dispersion when the emergent EM field is manually turned off by setting $\alpha_{i\varphi} = 1$ in Eq. (11). Without the emergent EM field, the dispersive edge bands expected for the induced $(p_r + ip_\varphi)$ -wave-like gap are evident, whereas in the presence of it the bulk gap is diminished, although the trace of edge bands can still be seen in some cases (compare $q_\varphi \approx 0$ and $E(n, q_\varphi) \approx 0$ regions in Fig. 2(d) and (e)).

The relevance of this pedagogical model is made clear by shrinking the spins at the $r_i = 0$ edge (green arrows in Fig. 2(a)) into one single spin, which results in a nonchiral skyrmion on a polar lattice shown in Fig. 2(b), with the same interface magnetic field described by Eq. (9). Certainly these two lattices cannot be mapped to each other exactly, but their low energy sectors display similar features.

The pedagogical model indicates that the SC/skyrmion interface hosts a complex interplay between (i) the s -wave gap, (ii) the induced $(p_r + ip_\varphi)$ -wave-like gap, (iii) the emergent EM field, and (iv) the $s-d$ coupling B_0 . Motivated by the STM generated single skyrmion [44] (although with an external magnetic field), we proceed to study the SC/skyrmion interface on a single open square (SC/SK), whose spin texture

\mathbf{B}_i at position $\mathbf{r}_i = (x_i, y_i) = |\mathbf{r}_i|(\cos\varphi_i, \sin\varphi_i)$, as shown in Fig. 2(c), is that described by Eq. (9), but with $\theta_i = \pi|\mathbf{r}_i|/R(\mathbf{r}_i)$. Here, $R(\mathbf{r}_i)$ is the length of the straight line that passes through \mathbf{r}_i connecting the center of the square with the edge. The spontaneous current at site i can be calculated from Eq. (1) by

$$\mathbf{J}_i = -i \sum_{\sigma\delta} t_\delta \delta \langle f_{i+\delta\sigma}^\dagger f_{i\sigma} \rangle. \quad (13)$$

As shown in Fig. 2(f) and (g), in the normal state (NM/SK) there is a persistent current whose vorticity strongly depends on the emergent EM field, the $s-d$ coupling B_0 , and finite chemical potential. Because the persistent current also has edge component, the topological edge current alone is hard to be quantified in the SC state from the pattern shown in Fig. 2(h) and (i). At $B_0 \gg \Delta$, the current pattern in the SC state recovers that of the NM state, as can be seen by comparing Fig. 2(g) and (i). For the chiral skyrmion seen in most experiments, the form of B^x and B^y in Eq. (9) are exchanged, which gives the same result as σ^x and σ^y can be trivially exchanged for spin-independent quantities such as \mathbf{J}_i . These results suggest a vortex-like state at the NM/skyrmion lattice or SC/skyrmion lattice interface, whose vorticity depends on material properties.

In summary, we propose that a broad class of non-collinear magnetic orders, including a large part of those discovered in multiferroic insulators, and the Bloch and Neel domain walls in collinear magnetic insulators, can be used to practically generate Majorana edge states at their interface to a conventional SC. The advantages of these systems include a much larger parameter space to stabilize the edge states compared to 1D proposals, the longer range magnetic order may help to separate the edge states over a macroscopic distance, and adjusting chemical potential is not necessary. The proximity to a skyrmion induces an inhomogeneous $(p_r + ip_\varphi)$ -wave-like pairing in the SC under the influence of an emergent electromagnetic field, and consequently a vortex-like state that features both a bulk persistent current and an edge current.

We thank P. W. Brouwer, Y.-H. Liu, and F. von Oppen for stimulating discussions.

-
- [1] C. Nayak, S. H. Simon, A. Stern, M. Freedman, and S. Das Sarma, Rev. Mod. Phys. **80**, 1083 (2008).
 - [2] J. Alicea, Reports on Progress in Physics **75**, 076501 (2012).
 - [3] C. Beenakker, Annual Review of Condensed Matter Physics **4**, 113 (2013).
 - [4] S. R. Elliott and M. Franz, Rev. Mod. Phys. **87**, 137 (2015).
 - [5] T. D. Stanescu and S. Tewari, J. Phys. Condens. Matter **25**, 233201 (2013).

- [6] A. P. Schnyder and P. M. R. Brydon, ArXiv e-prints (2015), 1502.03746.
- [7] A. Kitaev, *Physics Uspekhi* **44**, 131 (2001).
- [8] Y. Oreg, G. Refael, and F. von Oppen, *Phys. Rev. Lett.* **105**, 177002 (2010).
- [9] R. M. Lutchyn, J. D. Sau, and S. Das Sarma, *Phys. Rev. Lett.* **105**, 077001 (2010).
- [10] J. D. Sau, R. M. Lutchyn, S. Tewari, and S. Das Sarma, *Phys. Rev. Lett.* **104**, 040502 (2010).
- [11] V. Mourik, K. Zuo, S. M. Frolov, S. R. Plissard, E. P. A. M. Bakkers, and L. P. Kouwenhoven, *Science* **336**, 1003 (2012).
- [12] A. Das, Y. Ronen, Y. Most, Y. Oreg, M. Heiblum, and H. Shtrikman, *Nat. Phys.* **8**, 887 (2012).
- [13] T.-P. Choy, J. M. Edge, A. R. Akhmerov, and C. W. J. Beenakker, *Phys. Rev. B* **84**, 195442 (2011).
- [14] S. Nadj-Perge, I. K. Drozdov, B. A. Bernevig, and A. Yazdani, *Phys. Rev. B* **88**, 020407 (2013).
- [15] B. Braunecker and P. Simon, *Phys. Rev. Lett.* **111**, 147202 (2013).
- [16] F. Pientka, L. I. Glazman, and F. von Oppen, *Phys. Rev. B* **88**, 155420 (2013).
- [17] J. Klinovaja, P. Stano, A. Yazdani, and D. Loss, *Phys. Rev. Lett.* **111**, 186805 (2013).
- [18] M. M. Vazifeh and M. Franz, *Phys. Rev. Lett.* **111**, 206802 (2013).
- [19] F. Pientka, L. I. Glazman, and F. von Oppen, *Phys. Rev. B* **89**, 180505 (2014).
- [20] J. Röntynen and T. Ojanen, *Phys. Rev. B* **90**, 180503 (2014).
- [21] Y. Kim, M. Cheng, B. Bauer, R. M. Lutchyn, and S. Das Sarma, *Phys. Rev. B* **90**, 060401 (2014).
- [22] P. M. R. Brydon, S. Das Sarma, H.-Y. Hui, and J. D. Sau, *Phys. Rev. B* **91**, 064505 (2015).
- [23] L. Yu, *Acta Phys. Sin.* **21** (1965).
- [24] H. Shiba, *Progress of Theoretical Physics* **40**, 435 (1968).
- [25] A. I. Rusinov, *Zh. Eksp. Teor. Fiz. Pisma. Red.* **9**, 146 (1968).
- [26] S. Nadj-Perge, I. K. Drozdov, J. Li, H. Chen, S. Jeon, J. Seo, A. H. MacDonald, B. A. Bernevig, and A. Yazdani, *Science* **346**, 602 (2014).
- [27] J. D. Sau and P. M. R. Brydon, ArXiv e-prints (2015), 1501.03149.
- [28] S. Nakosai, Y. Tanaka, and N. Nagaosa, *Phys. Rev. B* **88**, 180503 (2013).
- [29] G. Deutscher and F. Meunier, *Phys. Rev. Lett.* **22**, 395 (1969).
- [30] J. J. Hauser, *Phys. Rev. Lett.* **23**, 374 (1969).
- [31] P. D. Gennes, *Physics Letters* **23**, 10 (1966), ISSN 0031-9163.
- [32] Y. Yamasaki, H. Sagayama, T. Goto, M. Matsuura, K. Hirota, T. Arima, and Y. Tokura, *Phys. Rev. Lett.* **98**, 147204 (2007).
- [33] Y. Yamasaki, H. Sagayama, N. Abe, T. Arima, K. Sasai, M. Matsuura, K. Hirota, D. Okuyama, Y. Noda, and Y. Tokura, *Phys. Rev. Lett.* **101**, 097204 (2008).
- [34] T. Kimura and Y. Tokura, *Journal of Physics: Condensed Matter* **20**, 434204 (2008).
- [35] H. Murakawa, Y. Onose, F. Kagawa, S. Ishiwata, Y. Kaneko, and Y. Tokura, *Phys. Rev. Lett.* **101**, 197207 (2008).
- [36] N. Sedlmayr, J. M. Aguiar-Hualde, and C. Bena, *Phys. Rev. B* **91**, 115415 (2015).
- [37] Y. Kajiwara, K. Harii, S. Takahashi, J. Ohe, K. Uchida, M. Mizuguchi, H. Umezawa, H. Kawai, K. Ando, K. Takanashi, et al., *Nature* **464**, 262 (2010).
- [38] R. D. Johnson, P. Barone, A. Bombardi, R. J. Bean, S. Picozzi, P. G. Radaelli, Y. S. Oh, S.-W. Cheong, and L. C. Chapon, *Phys. Rev. Lett.* **110**, 217206 (2013).
- [39] S. Seki, X. Z. Yu, S. Ishiwata, and Y. Tokura, *Science* **336**, 198 (2012).
- [40] S. Seki, S. Ishiwata, and Y. Tokura, *Phys. Rev. B* **86**, 060403 (2012).
- [41] T. Schulz, R. Ritz, A. Bauer, M. Halder, M. Wagner, C. Franz, C. Pfleiderer, K. Everschor, M. Garst, and A. Rosch, *Nat Phys* **8**, 301 (2012).
- [42] N. Nagaosa and Y. Tokura, *Nat Nano* **8**, 899 (2013).
- [43] S. Zhang and S. S.-L. Zhang, *Phys. Rev. Lett.* **102**, 086601 (2009).
- [44] N. Romming, C. Hanneken, M. Menzel, J. E. Bickel, B. Wolter, K. von Bergmann, A. Kubetzka, and R. Wiesendanger, *Science* **341**, 636 (2013).